

**Marcelo Augusto dos Reis,^a
 Antonio Marcos Saraiva,^b
 Marcelo Leite dos Santos,^a
 Anete Pereira de Souza^{b,c} and
 Ricardo Aparicio^{a*}**

^aLaboratory of Structural Biology and Crystallography, Institute of Chemistry, University of Campinas, CP 6154, 13084-862 Campinas-SP, Brazil, ^bPlant Biology Department, Biology Institute, University of Campinas, CP 6010, 13083-875 Campinas-SP, Brazil, and ^cGenetic and Molecular Analysis Laboratory, Molecular Biology and Genetic Engineering Center (CBMEG), University of Campinas, CP 6010, 13083-970 Campinas-SP, Brazil

Correspondence e-mail:
 aparicio@iqm.unicamp.br

Received 21 December 2011
 Accepted 16 February 2012

Crystallization and preliminary X-ray analysis of stationary phase survival protein E (SurE) from *Xylella fastidiosa* in two crystal forms

The bacterium *Xylella fastidiosa* is a phytopathogenic organism that causes citrus variegated chlorosis, a disease which attacks economically important crops, mainly oranges. In this communication, the crystallization and preliminary X-ray crystallographic analysis of XfSurE, a survival protein E from *X. fastidiosa*, are reported. Data were collected for two crystal forms, I and II, to 1.93 and 2.9 Å resolution, respectively. Crystal form I belonged to space group C2, with unit-cell parameters $a = 172.36$, $b = 84.18$, $c = 87.24$ Å, $\alpha = \gamma = 90$, $\beta = 96.59^\circ$, whereas crystal form II belonged to space group C2, with unit-cell parameters $a = 88.05$, $b = 81.26$, $c = 72.84$ Å, $\alpha = \gamma = 90$, $\beta = 94.76^\circ$.

1. Introduction

Xylella fastidiosa is the phytopathogen that causes citrus variegated chlorosis (CVC), a disease which attacks economically important crops: mainly oranges but also other crops including grapes (Lee *et al.*, 1991; Laranjeira, 1997). Fruits from affected trees ripen earlier with smaller size and hardness. Currently, the only remedy consists of palliative action, including the elimination of contaminated trees.

The *surE* gene is widely distributed among eubacteria (except for Gram-positive bacteria and mycobacteria), archaeobacteria and eukaryotes (Li *et al.*, 1994, 1997; Visick *et al.*, 1998). It is intensely transcribed in the stationary phase or under conditions of high cell density where there is a reduction in bacterial growth (Ichikawa *et al.*, 1994). The biochemical and physiological functions of SurE proteins are not fully known. They were initially classified as acid phosphatases (Zhang *et al.*, 2001) with a preference for purine nucleotides (Mura *et al.*, 2003) and as metal-dependent enzymes. Biochemical studies have shown that this enzyme can perform dephosphorylation of several ribonucleotides and of deoxyribonucleotide 5'-monophosphates and ribonucleoside 3'-monophosphates in *Escherichia coli*, and reclassification as a nucleotidase has been suggested (Proudfoot *et al.*, 2004). An additional hypothesis is that SurE proteins may be housekeeping enzymes that act in the dephosphorylation of non-canonical nucleosides which are potentially mutagenic to the cell (Gonçalves *et al.*, 2008; Galperin *et al.*, 2006).

The closest homologue of SurE from *X. fastidiosa* (XfSurE) studied by crystallographic techniques to date is SurE from *Salmonella typhimurium* (54% identity; Pappachan *et al.*, 2008). The tertiary structure of SurE essentially consists of two parts: a globular domain arranged as a Rossmann-like fold (three-layer $\alpha/\beta/\alpha$) and a β -hairpin that is supposed to mediate a tetrameric oligomer under physiological conditions. However, the biologically active form is still controversial and seems to be dependent on the organism being studied, with either dimers or tetramers (or both) being reported as the functional unit in solution (Lee *et al.*, 2001; Zhang *et al.*, 2001; Gonçalves *et al.*, 2008; Proudfoot *et al.*, 2004). Recently, we reported the cloning, expression, purification and structural characterization of XfSurE in solution, together with enzyme-kinetics studies (Saraiva *et al.*, 2009). Our results unequivocally indicated that XfSurE is a tetramer in solution and exhibits a highly positive cooperative behaviour between the catalytic subunits in the presence of natural substrates. In addition, a mechanism was proposed based on small-angle X-ray scattering (SAXS) experiments, in which it was hypothesized that domain movements in solution would allow XfSurE to perform allosteric



control during the dephosphorylation process. Crystallographic studies were initiated with the aim of providing high-resolution details from which further insights into the functional mechanism of XfSurE could be obtained. Here, we report the crystallization and preliminary X-ray crystallographic analysis of the gene product of ORF XF0703 (<http://www.xylella.lncc.br>), referred to as XfSurE, a protein with 263 amino acids and of molecular mass 28.3 kDa, in two different apo crystal forms.

2. Materials and methods

2.1. Cloning, expression and purification

The *surE* gene from *X. fastidiosa* was amplified by PCR using genomic DNA as a template. The reaction product of the amplification procedure was cloned into pET29a and transformed into *E. coli* DH5- α . The plasmid containing the *surE* insert was transformed into *E. coli* BL21 (DE3) cells, inoculated into 3 ml TB medium containing 40 $\mu\text{g ml}^{-1}$ kanamycin overnight at 310 K and 300 rev min^{-1} and transferred to 2 l TB with the same concentration of antibiotic. The cells were grown to an OD_{560} of 0.6–0.8, at which point protein overexpression was induced by addition of 5.6 mM lactose followed by cultivation for 20 h at 310 K and 300 rev min^{-1} . The culture was then centrifuged at 4200 rev min^{-1} for 15 min at 277 K and pelleted cells were resuspended in buffer A (50 mM Tris-HCl pH 7.5 with 300 mM NaCl) plus 1 mg ml^{-1} lysozyme and 1 mM phenylmethylsulfonyl fluoride (PMSF; Sigma Chemical, St Louis, Missouri, USA). The cell suspension was left to stand for 30 min at 277 K, followed by sonication. Clarification was performed twice by centrifugation at 15 000 rev min^{-1} for 40 min at 277 K. Purification of the XfSurE protein was performed in a single chromatography step using an Ni-NTA column (Qiagen, Hilden, Germany) equilibrated with buffer A. The purified protein was eluted with five column volumes of buffer A containing 250 mM imidazole and the purity was examined by SDS-PAGE. Subsequently, the purified XfSurE was dialyzed in buffer B (25 mM Tris-HCl, 50 mM NaCl, 1 mM DTT). All chemical reagents used were of the highest available grade.

2.2. Crystallization and data collection

Crystallization conditions were screened at 293 K using the commercially available kits Crystal Screen, Crystal Screen 2 and SaltRx (Hampton Research); Wizard I and II and Precipitant Synergy (Emerald BioSystems); and PACT and JCSG+ (NeXtal/Qiagen) with a Honeybee 963 Pipettor robot (Genomic Solutions) using the sitting-drop vapour-diffusion method in 96-well plates. To

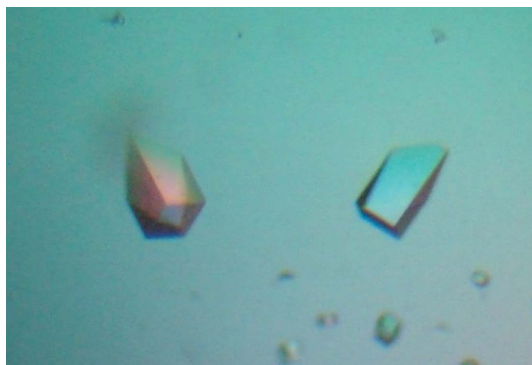


Figure 1
Typical crystals of XfSurE representing forms I and II. Maximum dimensions are $\sim 140 \times 70 \times 70 \mu\text{m}$.

obtain suitable crystals for X-ray diffraction experiments, the initial crystallization conditions were further improved by a conventional optimization approach based on screening of parameter values such as buffer pH, concentration of precipitant, salt and protein at 293 K by the hanging-drop vapour-diffusion method in Tissue Culture Test Plates 24 (TPP). The highest affinity XfSurE cofactor, Mn^{2+} (Saraiva *et al.*, 2009), was also added to some conditions during the optimization process. In addition, the use of additives and seeding techniques was adopted as a strategy in the search for better diffracting crystals. As a result, two different crystal forms were obtained which grew to full size within two weeks and exhibited very similar crystal habits, only being clearly distinguishable by X-ray analysis. Typical XfSurE crystals are shown in Fig. 1.

2.2.1. Crystal form I. Crystal form I was obtained using a reservoir solution (500 μl) consisting of 0.1 mM bis-tris propane (Sigma) pH 7.5, 0.14 M sodium iodide (Vetec), 20% (w/v) PEG 3350 (Sigma), 5 mM dithiothreitol (DTT) and 0.1 mM MnCl_2 (corresponding to a 2:1 stoichiometric ratio of XfSurE monomer and manganese ion in the droplet) mixed in equal amounts (2 μl :2 μl) with protein solution at a concentration of 6.1 mg ml^{-1} in the dialysis buffer. Diffraction data were collected at a wavelength of 1.459 Å using a MAR Mosaic CCD 225 detector on the W01B-MX2 beamline of the Laboratório Nacional de Luz Síncrotron (LNLS, Campinas, Brazil) by the oscillation method using a crystal-to-detector distance of 120 mm, a 25 s exposure time and 0.7° oscillation per frame to give a total of 330 images. A representative diffraction pattern from this data set is presented in Fig. 2. To prevent radiation damage, the crystal was soaked in a cryoprotectant solution supplemented with 20% (v/v) glycerol and flash-cooled in a nitrogen-gas stream at 100 K (Oxford Cryosystems).

2.2.2. Crystal form II. Crystal form II was produced under similar conditions to form I, in which a reservoir solution consisting of 0.1 mM bis-tris propane pH 7.6, 0.13 M sodium iodide, 16% (w/v) PEG 3350, 5 mM dithiothreitol (DTT) and 0.5 mM MnCl_2 (a 1:2

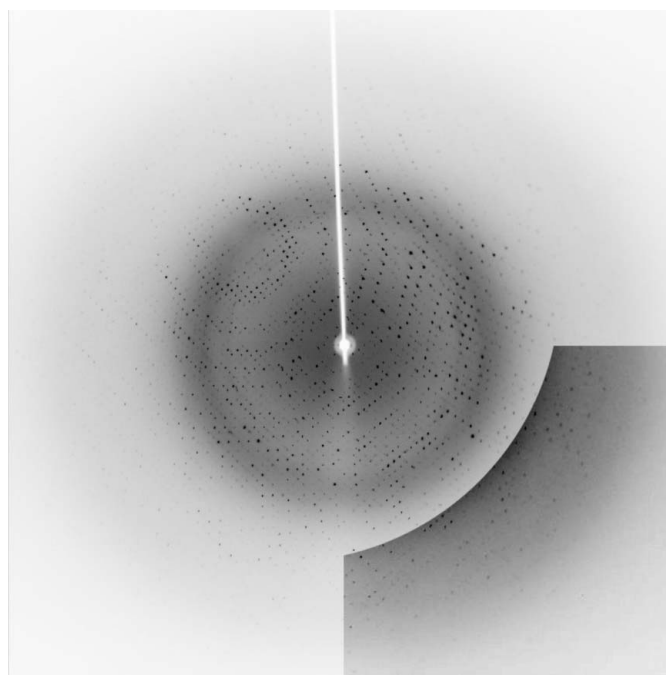


Figure 2
A diffraction pattern from crystal form I. The maximum resolution increases from 2 Å at the detector edge to 1.64 Å at the image corner. The contrast-enhanced region shows higher resolution diffraction spots.

stoichiometric ratio of XfSurE monomer:ion) was mixed in equal amounts with protein solution at 7.0 mg ml^{-1} . Various strategies were applied to overcome problems with ice formation during cooling, including the use of a number of alternative cryoprotectants and a gradual increase in their respective concentrations. Although grown under very similar conditions to crystal form I, the crystals of form II were very fragile and sensitive during transfer into cryoprotectant solutions. In spite of exhaustive attempts, we did not succeed in obtaining an efficient cooling protocol. The data set with the best statistics was collected by flash-cooling a crystal directly from the mother liquor in the nitrogen-gas stream (Oxford Cryosystems). The temperature was kept at 100 K during data collection. Data were collected on beamline D03B-MX1 of LNLS with a wavelength of 1.437 \AA using a crystal-to-detector distance of 85 mm, 240 s exposure time and 1.0° oscillation per frame. Images were recorded with a

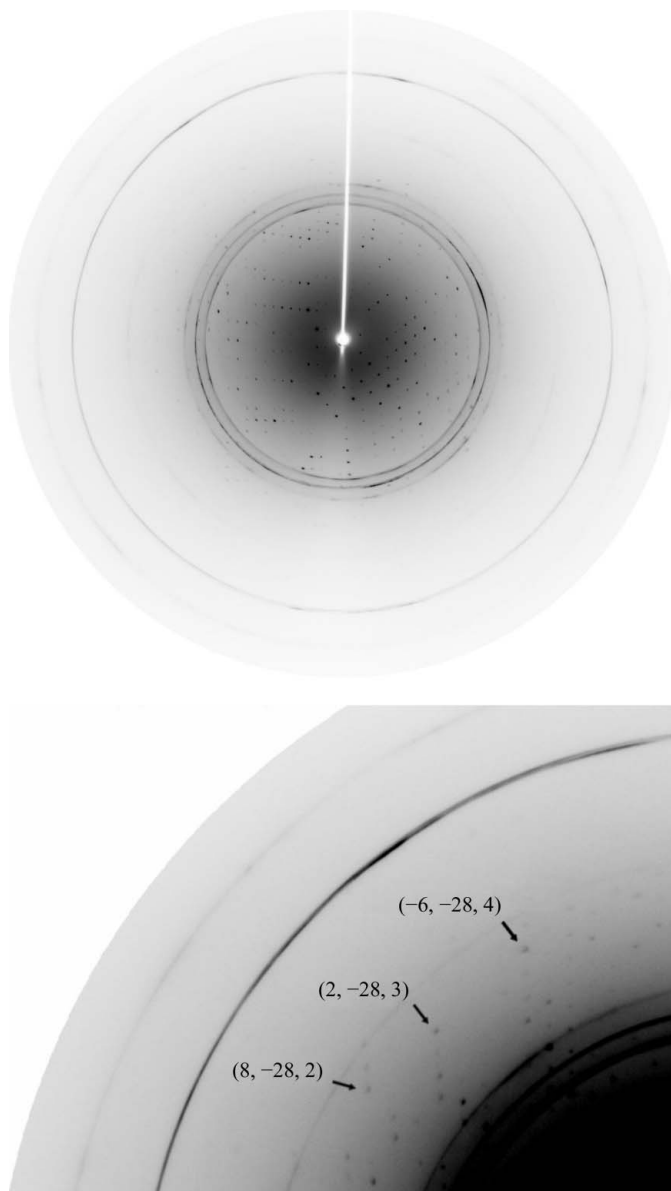


Figure 3 Representative diffraction pattern from the data set collected from crystal form II. For clarity, an enlarged region is presented along with higher resolution hkl reflections. The ice rings observed did not prevent successful data collection and structure determination.

Table 1 Statistics of data collection and processing.

Values in parentheses are for the highest resolution shell.

	Crystal form I	Crystal form II
Beamline	W01B-MX2	D03B-MX1
Wavelength (\AA)	1.459	1.437
No. of images	330	137
Space group	C2	C2
Unit-cell parameters (\AA , $^\circ$)	$a = 172.36$, $b = 84.18$, $c = 87.24$, $\beta = 96.59$	$a = 88.05$, $b = 81.26$, $c = 72.84$, $\beta = 94.76$
Solvent content (%)	53.86	44.14
Protomers in asymmetric unit	4	2
Resolution limits (\AA)	57–1.93 (2.03–1.93)	24.20–2.90 (3.06–2.90)
No. of reflections	412918 (52628)	27281 (4452)
Unique reflections	92203 (12675)	10399 (1663)
Multiplicity	4.5 (4.2)	2.6 (2.7)
Completeness (%)	98.9 (93.3)	90.9 (100.0)
R_{merge}^\dagger (%)	6.0 (45.2)	24.5 (71.9)
$\langle I/\sigma(I) \rangle$	17.3 (2.5)	2.8 (2.0)
Wilson plot B factor (\AA^2)	30.9	119.8

$^\dagger R_{\text{merge}} = \frac{\sum_{hkl} \sum_i |I_i(hkl) - \langle I(hkl) \rangle|}{\sum_{hkl} \sum_i I_i(hkl)}$, where $I_i(hkl)$ is the intensity of the i th observation of reflection hkl .

MAR Mosaic CCD 165 detector as a total of 137 images. Fig. 3 shows a representative diffraction image from this data set.

3. Results and discussion

Data reduction and analysis were performed using *MOSFLM* and *SCALA* and other programs from the *CCP4* suite (Winn *et al.*, 2011). Results of data processing and statistics are summarized in Table 1. The narrow resolution intervals corresponding to the ice rings observed in crystal form II were excluded during integration and scaling. In view of the availability of crystallographic structures of XfSurE homologues, molecular replacement was carried out using the automated procedure implemented in the *BALBES* package (Long *et al.*, 2008). The same program version and database were employed for crystal forms I and II in order to obtain comparable parameters. In both cases a solution was found. The *BALBES* protocol included 30 cycles of automated restrained refinement using *REFMAC* (Winn *et al.*, 2011). For crystal form I, based on the protein sequence, *BALBES* built 22 models comprising ten monomers, seven dimers and five tetramers. For form II, ten monomers and seven dimers were used, in a total of 17 models. In both cases, the successful search model was a dimer built from chains *A* and *B* of the PDB entry 2wqk (which superseded entry 2phj), which corresponds to a SurE protein from *Aquifex aeolicus* VF5 (Antonyuk *et al.*, 2009) and exhibits 42% identity with XfSurE.

The solution obtained for crystal form I consisted of a tetramer in the asymmetric unit. For this crystal form, decreases in the R factor from 51.5 to 37.6% and in R_{free} (5% of the total reflections) from 51.0 to 41.0% were observed and a *BALBES* Q factor parameter of 0.6982 was obtained. In the case of crystal form II, a dimer was found in the asymmetric unit; the R factor decreased from 48.9 to 38.9% and R_{free} decreased from 51.4 to 47.7%, with a Q factor of 0.5624. No steric clashes were observed in either case. Together, these results unequivocally indicate that the molecular-replacement procedure was successful for both crystal forms. Refinement of both structures is in progress.

Data from crystal form II were collected to a lower resolution limit compared with form I. The reason for the change in the content of the asymmetric unit from a tetramer to a dimer requires further analysis. In principle, it could be a result of the absence of a cryoprotectant agent in the drop solution or a simple consequence of different crystal

packing. However, it is worth noting that the manganese ion, a cofactor of SurE which probably binds in interface regions between the dimers that form the tetramer (as reported for other proteins in this family) is present in a higher amount in the growing solution of crystal form II. Therefore, it would also be possible that the observed difference might be related to the recently proposed and above-mentioned hypothesis of allosteric behaviour which includes domain movements (Saraiva *et al.*, 2009). In addition, attempts to obtain XfSurE with different ligands are in progress. Overall, comparative analysis of the refined apo structures together with the planned holo structures and the available structures of more distant protein homologues may make a valuable contribution to a better understanding of the subtle differences in the β -hairpin subdomains that are responsible for the oligomeric arrangement and that would be involved in allosteric control of the dephosphorylation process.

This work was supported by the Fundação de Amparo à Pesquisa do Estado de São Paulo (01/07533-7 to APS and 05/03234-6 to RA). MAR and MLS received PhD fellowships from the Conselho Nacional de Desenvolvimento Científico e Tecnológico (CNPq) and AMS from FAPESP. RA was also supported by a research grant from CNPq. We gratefully acknowledge the Laboratório Nacional de Luz Síncrotron (LNLS) for D03B-MX1 and W01B-MX2 beamline time as well for the use of the Honeybee 963 Pipettor robot facility and Professor Carol Collins (IQ/UNICAMP) for reading the manuscript and assisting with language revision.

References

- Antonyuk, S. V., Ellis, M. J., Strange, R. W., Bessho, Y., Kuramitsu, S., Shinkai, A., Yokoyama, S. & Hasnain, S. S. (2009). *Acta Cryst.* **F65**, 1204–1208.
- Galperin, M. Y., Moroz, O. V., Wilson, K. S. & Murzin, A. G. (2006). *Mol. Microbiol.* **59**, 5–19.
- Gonçalves, A. M. D., Rêgo, A. T., Thomaz, M., Enguita, F. J. & Carrondo, M. A. (2008). *Acta Cryst.* **F64**, 213–216.
- Ichikawa, J. K., Li, C., Fu, J. & Clarke, S. (1994). *J. Bacteriol.* **176**, 1630–1638.
- Laranjeira, F. F. (1997). *Laranja*, **18**, 123–141.
- Lee, R. F., Derrick, K. S., Beretta, M. J. G., Chagas, C. M. & Rosetti, V. (1991). *Citrus Ind.* **72**, 10–13.
- Lee, J. Y., Kwak, J. E., Moon, J., Eom, S. H., Liong, E. C., Pedelacq, J.-D., Berendzen, J. & Suh, S. W. (2001). *Nature Struct. Biol.* **8**, 789–794.
- Li, C., Ichikawa, J. K., Ravetto, J. J., Kuo, H.-C., Fu, J. C. & Clarke, S. (1994). *J. Bacteriol.* **176**, 6015–6022.
- Li, C., Wu, P.-Y. & Hsieh, M. (1997). *Microbiology*, **143**, 3513–3520.
- Long, F., Vagin, A. A., Young, P. & Murshudov, G. N. (2008). *Acta Cryst.* **D64**, 125–132.
- Mura, C., Katz, J. E., Clarke, S. G. & Eisenberg, D. (2003). *J. Mol. Biol.* **326**, 1559–1575.
- Pappachan, A., Savithri, H. S. & Murthy, M. R. N. (2008). *FEBS J.* **275**, 5855–5864.
- Proudfoot, M., Kuznetsova, E., Brown, G., Rao, N. N., Kitagawa, M., Mori, H., Savchenko, A. & Yakunin, A. F. (2004). *J. Biol. Chem.* **279**, 54687–54694.
- Saraiva, A. M., Reis, M. A., Tada, S. F., Rosselli-Murai, L. K., Schneider, D. R., Pellosso, A. C., Toledo, M. A., Giles, C., Aparicio, R. & de Souza, A. P. (2009). *FEBS J.* **276**, 6751–6762.
- Visick, J. E., Ichikawa, J. K. & Clarke, S. (1998). *FEMS Microbiol. Lett.* **167**, 19–25.
- Winn, M. D. *et al.* (2011). *Acta Cryst.* **D67**, 235–242.
- Zhang, R. G., Skarina, T., Katz, J. E., Beasley, S., Khachatryan, A., Vyas, S., Arrowsmith, C. H., Clarke, S., Edwards, A., Joachimiak, A. & Savchenko, A. (2001). *Structure*, **9**, 1095–1106.